CHEMISTRY
A EUROPEAN JOURNAL

DOI: 10.1002/chem.201001032

Towards a Molecular Understanding of Cation–Anion Interactions—Probing the Electronic Structure of Imidazolium Ionic Liquids by NMR Spectroscopy, X-ray Photoelectron Spectroscopy and Theoretical Calculations

Till Cremer,[a] Claudia Kolbeck,[a] Kevin R. J. Lovelock,[b] Natalia Paape,[c] René Wölfel,[c] Peter S. Schulz,[c] Peter Wasserscheid,[c] Henry Weber,[d] Jens Thar,[d] Barbara Kirchner,[d] Florian Maier,*[a] and Hans-Peter Steinrück[a]

Abstract: Ten $[C_8C_1Im]^+$ (1-methyl-3-octylimidazolium)-based ionic liquids with anions Cl^-, Br^-, I^-, $[NO_3]^-$, $[BF_4]^-$, $[TfO]^-$, $[PF_6]^-$, $[Tf_2N]^-$, $[Pf_2N]^-$, and $[FAP]^-$ (TfO = trifluoromethylsulfonate, Tf_2N = bis(trifluoromethylsulfonyl)imide, Pf_2N = bis(pentafluoroethylsulfonyl)imide, FAP = tris(pentafluoroethyl)trifluorophosphate) and two $[C_8C_1C_1Im]^+$ (1,2-dimethyl-3-octylimidazolium)-based ionic liquids with anions Br^- and $[Tf_2N]^-$ were investigated by using X-ray photoelectron spectroscopy (XPS), NMR spectroscopy and theoretical calculations. While ^1H NMR spectroscopy is found to probe very specifically the strongest hydrogen-bond interaction between the hydrogen attached to the C^2 position and the anion, a comparative XPS study provides first direct experimental evidence for cation–anion charge-transfer phenomena in ionic liquids as a function of the ionic liquid's anion. These charge-transfer effects are found to be surprisingly similar for $[C_8C_1Im]^+$ and $[C_8C_1C_1Im]^+$ salts of the same anion, which in combination with theoretical calculations leads to the conclusion that hydrogen bonding and charge transfer occur independently from each other, but are both more pronounced for small and more strongly coordinating anions, and are greatly reduced in the case of large and weakly coordinating anions.

Keywords: charge transfer · density functional calculations · electronic interactions · ionic liquids · NMR spectroscopy · X-ray photoelectron spectroscopy

Introduction

Ionic liquids (ILs), salts with a melting point below 100 °C, have shown great promise in both experimental and theoretical environments in the last decade.[1] There are at least 10^6 potential primary ILs, of which many have very interesting physicochemical properties, leading to a burgeoning area of research and industrial applications, such as the BASIL (biphasic acid scavenging utilising ionic liquids) process.[2] ILs have even been labelled "designer solvents" for the exciting prospect of tailoring their physical properties by combining the appropriate cations and anions with their individual properties as building blocks to obtain the desired IL. Indeed, it has been shown that trends for groups of compounds exist making the prediction of physical and chemical properties for a chosen combination of cation and anion feasible to a certain extent.[3,4] However, the simple picture of superimposing properties of the individual ions does not hold true. Anion and cation will always interact in a specific way leading to a unique combination with specific proper-

[a] T. Cremer, C. Kolbeck, Dr. F. Maier, Prof. Dr. H.-P. Steinrück
Lehrstuhl für Physikalische Chemie II
Universität Erlangen-Nürnberg, Egerlandstrasse 3
91058 Erlangen (Germany)
Fax: (+49) 9131-85-28867
E-mail: florian.maier@chemie.uni-erlangen.de

[b] Dr. K. R. J. Lovelock
School of Chemistry, The University of Nottingham
Nottingham, NG7 2RD (UK)

[c] N. Paape, R. Wölfel, Dr. P. S. Schulz, Prof. Dr. P. Wasserscheid
Lehrstuhl für Chemische Reaktionstechnik
Universität Erlangen-Nürnberg, Egerlandstrasse 3
91058 Erlangen (Germany)

[d] H. Weber, J. Thar, Prof. Dr. B. Kirchner
Wilhelm-Ostwald-Institut für Physikalische und Theoretische Chemie
Linnéstraße 2, 04103 Leipzig (Germany)

Supporting information for this article is available on the WWW under http://dx.doi.org/10.1002/chem.201001032.

ties. In order to evaluate the predictive power and the uncertainties of this "superposition" approach, one has to understand the nature of different interactions between cation and anion in any given IL. Apart from coulomb forces, dispersive and inductive interactions as well as hydrogen-bonding-type interactions play a considerable role in ILs.[5,6] In particular for the intensively studied class of imidazolium-based ILs, many groups have tried to qualitatively (and in some cases also quantitatively) correlate interactions between the ions with the physicochemical properties of the IL.[7–14] Due to the IL's ionic nature, coulombic interactions are expected to play a pronounced role. Commonly, the excess charges of the ions are considered to be integer values, that is, +1e for the imidazolium cation; within the last years a number of molecular dynamic (MD) simulations have been successfully carried out applying IL force fields with the constraint of integer-charged imidazolium cations and anions.[15–17] However, it was also shown that modified force fields with reduced (i.e., non-integer or fractional) charges on the ions considerably improve the MD results;[18,19] for details see the excellent review by Maginn.[20] When introducing such "effective charges" in computational chemistry, one might ask whether the value of this effective charge of a certain ion is a "real" quantity, implying some charge transfer between anion and cation, or whether it should be considered as a MD simulation parameter taking many body effects (e.g. polarisation) into account.[8,19,21,22] An indication of "real" fractional charges is provided by density functional theory (DFT) calculations. By applying a natural bond orbital (NBO) analysis of isolated ion pairs in their calculations, Hunt and co-workers observed a pronounced partial charge transfer between $[C_4C_1Im]^+$ and its counterion Cl^-.[8] Similar charge-transfer effects were already observed in DFT calculations of Na^+/Cl^- ion pairs.[23] A first step towards experimental evidence for non-integer charges was made by Tokuda et al., who introduced the parameter "effective ionic concentration", C_{eff}, in their combined electrochemical impedance and NMR measurements. This parameter was proposed to be dominantly related to the coulombic forces in the IL and to depend particularly on the nature of the anion and the chain length.[24] However, it does not only include contributions from effective ionic charges, but also takes into account ion aggregation (or dissociativity) as discussed in the concept of ionicity.[25] To the best of our knowledge a direct experimental proof of "reduced" or "effective" ionic charges in the case of ILs has not been reported yet.

A major point in the context of intermolecular forces in imidazolium based ILs is the elucidation of hydrogen bonding.[26] They mainly occur at the protons bound in C^2 and also—to a smaller extent—at the protons bound in C^4 and C^5 positions at the imidazolium ring (see Scheme 1). Hydrogen bonding has been proposed to be of crucial importance for the melting point as well as the viscosity of ILs.[12,14,27,28] While early experiments from Elaiwi et al.[27] and Avent et al.[28] indicate that less hydrogen bonding leads to a reduction in melting point and viscosity, more recent IR results

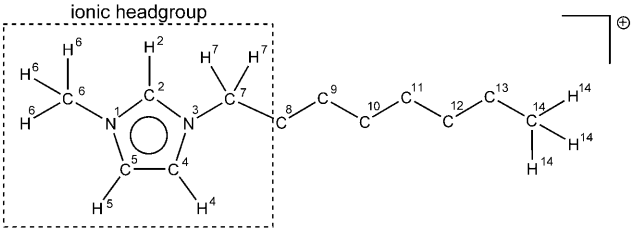

Scheme 1. Labelled structure of the $[C_8C_1Im]^+$ ion. The labelling method is the same as used by Hunt et al.[22] Carbon atoms attached to the ring of the ionic headgroup (C^2, C^4, C^5, C^6, C^7) are labelled in the text as "C_{hetero}" and C^8–C^{14} as "C_{alkyl}". Additionally, hydrogen atoms relevant for this work are added for sake of clarity.

and DFT calculations from the Ludwig group point towards a reverse trend.[12,14] In the last years, a large number of studies concerning hydrogen bonding in ILs have been carried out, mostly by NMR spectroscopy.[9–11,29,30] Lungwitz et al. correlated the Kamlet–Taft parameters α and β, which are well-known indicators for the hydrogen-bonding abilities of compounds, to ^1H NMR shifts of the proton bound to C^2. Their studies indicate that anion-dependent differential ^1H NMR shifts are a direct measure of the strength of hydrogen bonding in imidazolium-based ILs.[9,10] Most NMR studies mentioned above were carried out for ILs diluted in organic solvents, which has an influence on the NMR shifts.[28] However, ILs of sufficiently low viscosity can also be studied in undiluted pure form by NMR spectroscopy, thus ruling out additional solvent interactions that may complicate the interpretation of the obtained spectra.[31]

Finally, apart from coulombic and hydrogen-bonding interactions, dispersion and induction forces also significantly contribute to the specific interactions between anion and cation.[5] From ab inito calculations, considerable differences between ILs and classical molten salts were found due to different dispersive and inductive contributions, which may be an explanation for the reduced melting points and viscosities of ILs.[5]

Interactions between IL ions are closely related to their electronic structure. A very powerful experimental method in this respect is photoelectron spectroscopy (PES), which provides direct access to the electronic structure of a compound. Traditionally applied to solid surfaces, PES of ILs has only emerged during the last few years. Due to the very low vapour pressure of aprotic ILs (usually $<10^{-10}$ mbar at RT), PES is highly suitable for probing their electronic structure under ultra-high vacuum (UHV) conditions.[32–34] By means of ultra-violet photoelectron spectroscopy (UPS)[35–37] and inverse photoelectron spectroscopy (IPES),[36] occupied and unoccupied valence states are directly accessible. In combination with theory, the density of valence states ascribed to the cation and the anion have been successfully investigated.[35–37] Moreover, using X-ray photoelectron spectroscopy (XPS) core levels can be studied[35,37–48] and by analysing the so-called chemical shifts the different chemical environments of one specific element can be identified and quantified.[49] The binding energy (BE) of

a certain core level is a function of the chemical environment of the atom, that is, the oxidation state and the nature of the neighbouring atoms. In a simplified picture, the same core level of a given atom exhibits a higher BE if it is positively charged compared to a more negatively charged one. However, up to now, most XPS studies of pure ILs have concentrated on the surface composition and molecular orientation of the ions,[38,39,41,43,50–52] while few have addressed the electronic structure in terms of ion–ion interactions.[53]

To provide a more detailed understanding of the specific interactions within imidazolium-based ILs, we present here a systematic XPS and NMR study in combination with theoretical calculations. Pure ILs carrying the same cation, 1-methyl-3-octyl-imidazolium ($[C_8C_1Im]^+$), but ten different anions have been investigated (see Table 1). The $[C_8C_1Im]^+$ ion was chosen, because it has already been investigated in angle-resolved XPS studies with respect to molecular orientation effects at the surface.[50,51] It consists of a positively charged head group, that is, the imidazolium ring, and a neutral aliphatic tail. This pronounced asymmetry of the cation is one reason for the low melting point of all ILs investigated here.[2] The anions were selected due to the fact that they form room temperature ILs with the $[C_8C_1Im]^+$ ion, cover different sizes (ranging from Cl^- to $[FAP]^-$; FAP = tris(pentafluoroethyl)trifluorophosphate), different basicities, shapes (from spherical to elongated anions) and coordination abilities (from strongly coordinating halides to weakly coordinating anions with perfluoroalkyl groups), and

Table 1. Summary of ILs investigated in this study.

Chemical formula	Structure	Name
$[C_8C_1Im]Cl$	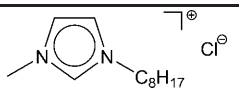	1-methyl-3-octylimidazolium chloride
$[C_8C_1Im]Br$	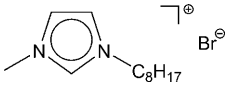	1-methyl-3-octylimidazolium bromide
$[C_8C_1Im]I$	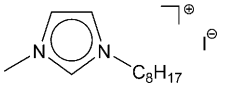	1-methyl-3-octylimidazolium iodide
$[C_8C_1Im][NO_3]$	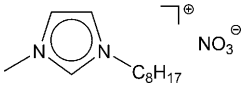	1-methyl-3-octylimidazolium nitrate
$[C_8C_1Im][BF_4]$	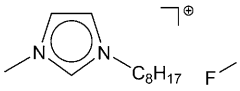	1-methyl-3-octylimidazolium tetrafluoroborate
$[C_8C_1Im][PF_6]$	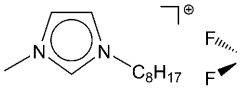	1-methyl-3-octylimidazolium hexafluorophosphate
$[C_8C_1Im][TfO]$	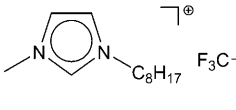	1-methyl-3-octylimidazolium trifluoromethylsulfonate
$[C_8C_1Im][Tf_2N]$	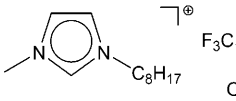	1-methyl-3-octylimidazolium bis[(trifluoromethyl)sulfonyl]imide
$[C_8C_1Im][Pf_2N]$	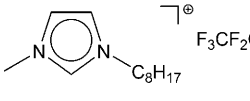	1-methyl-3-octylimidazolium bis[(pentafluoroethyl)sulfonyl]imide
$[C_8C_1Im][FAP]$	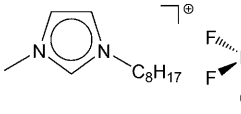	1-methyl-3-octylimidazolium tris(pentafluoroethyl)trifluorophosphate
$[C_8C_1C_1Im]Br$	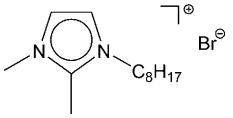	1,2-dimethyl-3-octylimidazolium bromide
$[C_8C_1C_1Im][Tf_2N]$	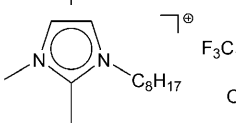	1,2-dimethyl-3-octylimidazolium bis[(trifluoromethyl)sulfonyl]imide

are free of aliphatic chains to avoid pronounced dispersive interactions with the chains of the cation. Moreover, the selected anions do not contain atoms that interfere with XPS and NMR signals from the cation and thus could complicate an unambiguous interpretation of the spectra. In addition, two ILs with the cation $[C_8C_1C_1Im]^+$ (methylated at the C^2-position) were compared to their unmethylated homologues.

Altogether, we will show that 1) the nature of the anion has a strong influence on the positive charge of the imidazolium ring, 2) that the absolute value of the positive charge on the imidazolium ring is hardly influenced by hydrogen-bonding interactions between anion and cation and 3) that the nature of the anion presumably modifies the degree of hybridisation in the imidazolium ring in case of the $[C_8C_1Im]^+$ ILs.

Results and Discussion

XPS measurements and computational results: The XPS data for all ten $[C_8C_1Im]^+$ ILs has been published previously in the context of surface composition and molecular orientation.[39,41,46,50,51,67] The XPS intensities of all ILs correspond within the margins of error with the nominal IL compositions confirming the high purity of the samples. Values for the elemental composition and BE values for all relevant core levels of all ILs are provided in Tables S1 and S2 in the Supporting Information. All ILs were free of surface contaminants.[42,43] Since this study focuses on the influence of the anion on the electronic structure of the imidazolium ring of the cation, only the C 1s and N 1s spectra will be discussed.

As already mentioned, direct comparison of absolute BE values is not possible due to minor charging effects in the range of ± 0.15 eV, which have been observed for all ILs (see Table S2 and Figure S1 in the Supporting Information). Slight charging of IL films during XPS was first observed and discussed by Smith et al.[39] As a consequence it is difficult to determine absolute BE values, in particular as no reference level (such as a Fermi edge) is available. To allow for a comparison of different ILs, one can choose a specific carbon atom as internal reference. Smith et al. arbitrarily chose the BE position of the C^2 carbon as internal reference. However, this approach proved to be impracticable for the present study, because the imidazolium ring interacts electronically with the anion (as will be shown in this paper). Therefore, we used the aliphatic carbon signal C_{alkyl} of the octyl chain, which is common to all ILs studied, as internal reference. After fitting the C 1s spectra, the C_{alkyl} BE position was set to (the arbitrarily chosen position of) 285.0 eV; this value is commonly used in XPS for adventitious hydrocarbon.[68] It should be mentioned here that the absolute calibration of the energy scale does not have an impact on the conclusions drawn from our data.

We justify our use of C_{alkyl} as reliable internal BE reference by the following reasons:

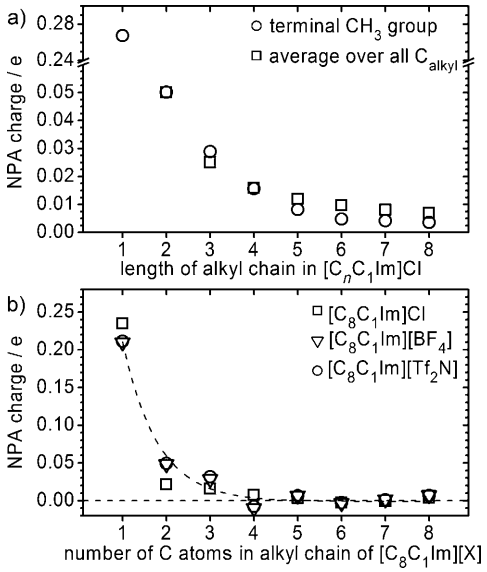

Figure 1. a) NPA charge of terminal CH_3 group (squares) and averaged NPA charge per CH_x unit of the alkyl chain (circles) of $[C_nC_1Im]Cl$ (in which $n=1$–8) as a function of chain length; b) NPA charges on the (CH_2) moieties and on the terminal CH_3 group of the octyl chain as a function of position and anion ($[C_8C_1Im]Cl$ squares; $[C_8C_1Im][BF_4]$ triangles, $[C_8C_1Im][Tf_2N]$ circles). The dashed line is an exponential fit to the mean values.

1) The aliphatic chain is expected to be least susceptible to chemical shifts due to the lack of coulombic interactions with the anion. It has been even shown that polar and non-polar regions are formed in long chained ILs, with the alkyl chains being on average separated from the ionic moieties.[69]
2) The ionic moieties (the charged imidazolium ring and the anion) most likely exhibit the strongest interactions as suggested by other groups.[8,11,70]
3) In an extended study of a series of $[C_nC_1Im][Tf_2N]$ with varying alkyl chain lengths it was found that the XPS peak separation Δ(BE) of the cationic carbon atoms, C_{hetero} and C_{alkyl}, remains unchanged for chains longer than C_8, meaning that from C_8 onwards the BE of C_{alkyl} is independent of the electronic structure and environment of the charged imidazolium ring.[46] This is further corroborated by calculations of a series of $[C_nC_1Im]Cl$ ($n=1$–8) showing the rapid decay of the positive charge with increasing chain length saturating around $n=8$: In Figure 1a the average NPA charge, as deduced by natural population analysis, per CH_x group ($x=2$, 3) of the alkyl chain and the NPA charge on the terminal CH_3 group of the alkyl chain are plotted as a function of chain length.
4) For the octyl chain as shown in Figure 1b for the three calculated $[C_8C_1Im]X$ ion pairs, the NPA charges on the (CH_2) units exhibit a fast drop to zero as a function of distance from the imidazolium ring, irrespective of the counterion. The exponential decay length is in the order of one C–C bond length, proving that the positive

charge on the imidazolium ring does not significantly impact on longer alkyl chains.

5) Finally, for practical reasons, the position of the dominant C_{alkyl} peak in the C 1s region can be determined with a high accuracy of better than 0.02 eV in our XPS measurements.

$[C_8C_1Im]^+$-based ILs: The C 1s spectra of all $[C_8C_1Im]^+$-based ILs are displayed in Figure 2. Common to all ILs is the dominant C_{alkyl} peak at 285.0 eV, which arises from the seven carbon atoms of the alkyl chain (see fit analysis in Table S1 in the Supporting Information). The second feature in the C 1s region is the peak/shoulder at 1.44 to 2.04 eV higher BE than the C_{alkyl} peak. This signal corresponds to the five carbon atoms bound to the nitrogen atoms of the imidazolium ring.

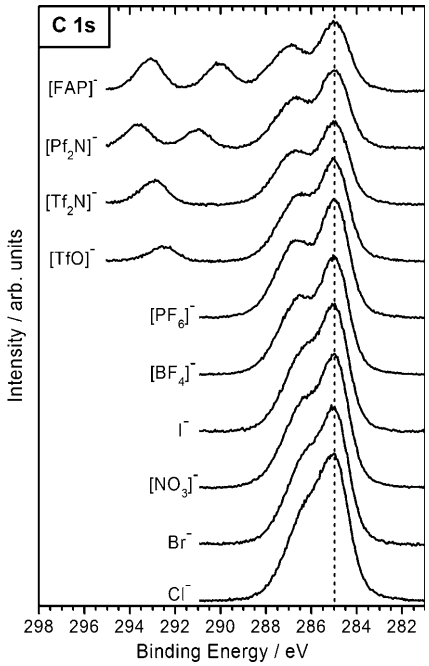

Figure 2. C 1s core level spectra of the ten $[C_8C_1Im]^+$ ILs investigated. BE scale is referenced to $BE(C_{alkyl}) = 285.0$ eV.

Further carbon signals at higher BE are observed for $[C_8C_1Im][Tf_2N]$ (peak at 293.0 eV), $[C_8C_1Im][Pf_2N]$ (peaks at 293.6 and 291.0 eV) and $[C_8C_1Im][FAP]$ (peaks at 293.3 and 291.0 eV). They correspond to the perfluorated carbon atoms of the anions with specific local electronic environments (see also Table S2).

Figure 3a shows a close-up of the cation-related C 1s signals. Inspection of this figure and of the fit results in Table S2 in the Supporting Information reveals that the C_{hetero} peak is subject to a differential shift with respect to the C_{alkyl} peak, depending on the nature of the anion. The shift follows a clear trend, from small peak separation $BE(C_{hetero}) - BE(C_{alkyl})$ of 1.44 eV for the smallest, most basic and most coordinating anion (Cl^-) to a considerably larger value of 2.04 eV for the much larger, least basic and least coordinating $[FAP]^-$ ion. The corresponding N 1s spectra are displayed in Figure 3b. For all ILs a symmetric peak is observed around 402 eV, which corresponds to the two nitrogen atoms of the imidazolium ring; these nitrogen atoms are indistinguishable with XPS.[38,39,41,42,46] Two of the ILs, $[C_8C_1Im][Tf_2N]$ and $[C_8C_1Im][Pf_2N]$, contain nitrogen in the anion with an extra N 1s peak at 399.6 eV, in accordance with previous publications.[50,51] The exact BE of the peak at $\approx$402 eV depends on the nature of the anion and follows the trend observed for C_{hetero} in the C 1s region (see Fig-

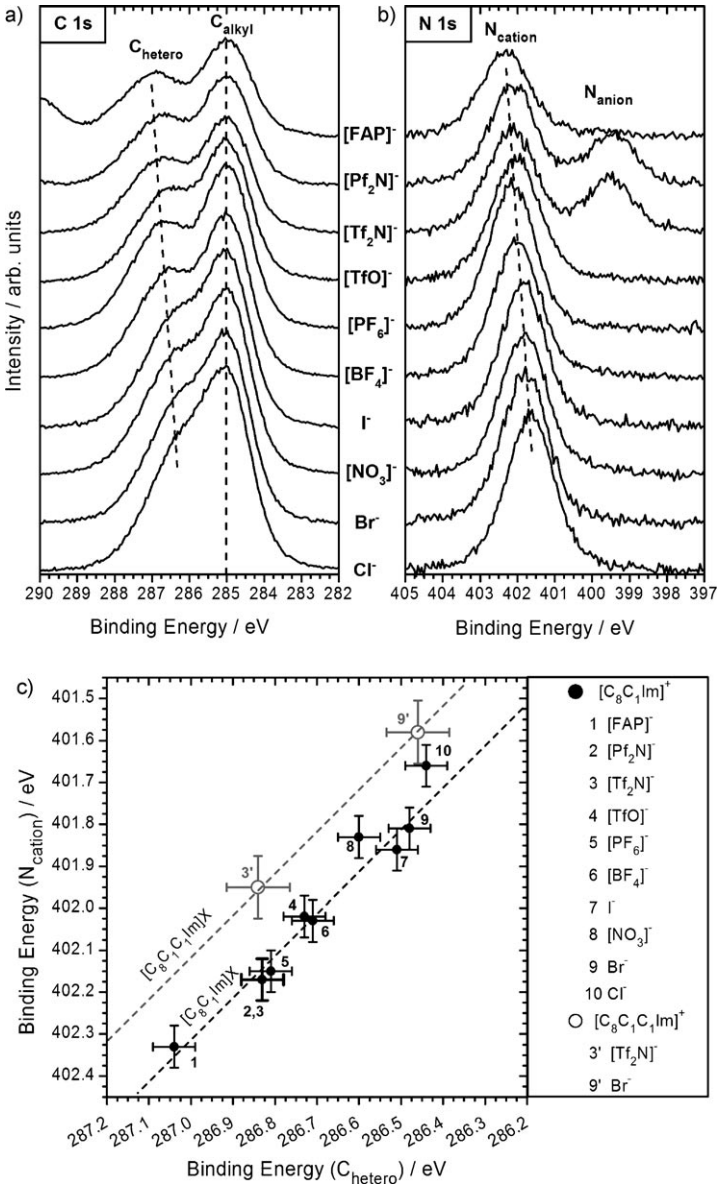

Figure 3. Detailed XP spectra of a) the C 1s and b) the N 1s regions for all $[C_8C_1Im]^+$ ILs (the dashed lines are guide to the eyes for the BE changes of the imidazolium ring signals). c) Correlation of BE positions for C_{hetero} and N_{cation} for the ten $[C_8C_1Im]^+$ ILs (filled) and the two $[C_8C_1C_1Im]^+$ ILs (hollow). Dashed lines with slope one are indicated for both groups.

ure 3a and 3b). In particular, the observed differential BE shifts of the imidazolium ring signals for each IL are more or less identical for both C 1s and N 1s regions. This is evident from Figure 3c, in which a linear relation between the C_{hetero} 1s and N 1s BE shifts with slope one is observed. This observation provides strong evidence that the shifts discussed above are genuine physical observables and not artefacts of the fitting procedure.

The observed differential shifts indicate that the nature of the anion must have an effect on the electronic structure of the counterion's imidazolium ring. In particular, for the smallest and most coordinating anions, the ring signals have the lowest binding energies and, vice versa, the highest BE values are measured for the largest and least coordinating anions. In Figure 4a and 4b the position of the C 1s and N 1s signals of the imidazolium ring are plotted against the IL molecular volume, demonstrating this general trend. From the smallest, most basic and most coordinating Cl^- ion up to the medium sized, weakly coordinating $[PF_6]^-$ ion the shift towards higher BE is nearly linear. Interestingly, for the three ILs containing $[PF_6]^-$, $[Tf_2N]^-$ and $[Pf_2N]^-$ (circles) the BE values are nearly constant, despite strong differences in molecular volume. This indicates that the coordination properties (all three anions are similarly very weakly coordinating) have the main effect on the BE shift. Apart from the size of the anion, other parameters describing the coordination behaviour were correlated with the observed anion-dependent BE shifts. As it is shown in Figure 4c and will be discussed in detail later, the BE shifts exhibit a linear relationship with the Kamlet Taft parameter β, which is a measure for the hydrogen-bond acceptor basicity of the IL anion.[9,71]

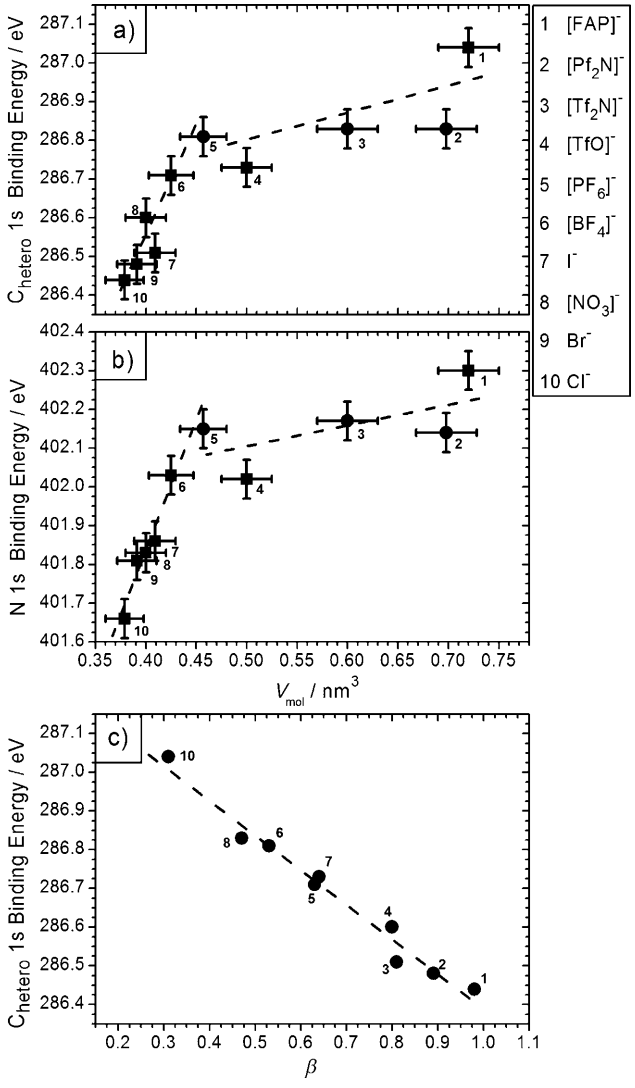

Figure 4. Correlation of BE values of a) C_{hetero} 1s and b) N_{cation} 1s of the ten $[C_8C_1Im]^+$-based ILs with molecular volume. Differentiation between squares and circles are for guidance to the eye according to the text. c) Correlation of C_{hetero} 1s BE with Kamlet–Taft parameter β (values for $[C_8C_1Im]Cl$, $[C_8C_1Im]Br$ and $[C_8C_1Im][FAP]$ are unpublished data from the Spange group, remaining values from reference [71]).

$[C_8C_1C_1Im]^+$-based ILs: Apart from coulombic forces, hydrogen-bonding interactions between cation and anion play a major role for imidazolium-based ILs;[9,10] they are mediated through the hydrogen atoms at the C^2, C^4 and C^5 positions (see also Scheme 1), with the hydrogen atom at C^2 contributing most (see also next section).[7,14,27,28,70] To study the possible influence of hydrogen bonding on the C_{hetero} 1 s BE discussed in the preceding paragraph, two representative ILs, namely $[C_8C_1C_1Im]Br$ and $[C_8C_1C_1Im][Tf_2N]$, in which a methyl group in C^2-position replaces the most acidic proton, were measured. Hence, hydrogen bonds between anions and cations are strongly reduced in these two ILs compared to their non-methylated homologues $[C_8C_1Im]Br$ and $[C_8C_1Im][Tf_2N]$.[7,72,73]

In Figure 5, the C 1s and N 1s spectra of the methylated ILs $[C_8C_1C_1Im][Tf_2N]$ (top) and $[C_8C_1C_1Im]Br$ (bottom) are displayed (black circles); for the C 1s region the spectra of the corresponding $[C_8C_1Im]^+$ ILs are superimposed (open circles). The BE of the N 1s signal from the methylated imidazolium ring exhibits an anion-dependent difference of 0.41 eV (Figure 5, right-hand side), which is within the margins of error nearly identical to the differential N 1s shift of 0.36 eV for the non-methylated homologues $[C_8C_1Im][Tf_2N]$ and $[C_8C_1Im]Br$ (Figure 3c and Table S2 in the Supporting Information); only the absolute value of the N 1s BE for the $[C_8C_1C_1Im]^+$ ILs is smaller by 0.2 eV (see also Figure 3c). In the C 1s spectra of both $[C_8C_1C_1Im]^+$ ILs the signal of the additional CH_3 group, with its BE between C_{hetero} and C_{alkyl}, is superimposed making the data interpretation not as straight forward as in the N 1s region. Nevertheless, the BE positions of C_{hetero} for both $[C_8C_1C_1Im]^+$ ILs can unambiguously be derived by fitting as shown in Figure 5 (left-hand side), and also by simple subtraction techniques (see Figure S2 in the Supporting Information). Independent of the presence of the methyl group in the C^2 position, the BE values of C_{hetero} for the Br^- as well as the $[Tf_2N]^-$ ILs are identical within ± 0.05 eV. These data demonstrate that the observed anion-dependent differential XPS shifts of the imidazolium ring signals are almost independent of the strength of the hydrogen bonding between anion and cation.

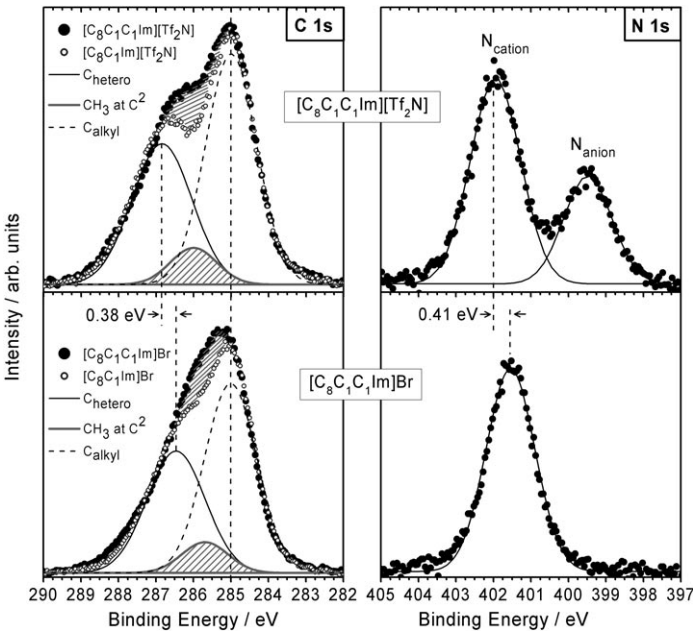

Figure 5. Analysis of C 1s and N 1s spectra of $[C_8C_1C_1Im][Tf_2N]$ and $[C_8C_1C_1Im]Br$. The grey fit curve corresponds to the contribution of the additional methyl group in C^2 position. The C 1s spectra of the two corresponding $[C_8C_1Im]^+$ ILs (open circles) are overlaid for comparison and illustration of the C^2-methyl contribution.

Interpretation of anion-dependent differential XPS shifts of imidazolium ring signals: In general, variations in the local electron density at a particular atom contribute to shifts in the corresponding core levels in XPS, the so-called chemical shifts. As a common trend, an increase in electron density at the atom under investigation (e.g., induced by electron transfer due to reduction or by bonding to an electron-donating neighbour atom) leads to a lowering of the measured core level BE, whereas a decrease in electron density (e.g., due to oxidation processes or due to bonding to an electron-withdrawing neighbour atom) increases the measured BE. In particular, very good correlation between XPS shifts and (semi)empirical charges on the atoms (e.g., described by oxidation states or Pauling charges) can be found, as already pointed out by the pioneering work of Siegbahn and coworkers.[74] For an accurate calculation of chemical shifts using ab initio methods, the discrimination between initial state effects (i.e., changes of the ground state) and final state effects (due to the specific response of the remaining electrons to screen the generated core hole during the photoemission process) is required, which is not straightforward at all. Fortunately, initial and final state effects in most cases result in BE shifts in the same direction,[49,75] which leads to the general observation that an increase of electron density at an atom yields a core-level shift towards lower binding energies (and vice versa).

Hence, we propose that our observed anion-dependent XPS shifts of the cationic headgroup are attributed to an anion-dependent transfer of charge between the anion and the cation. Such charge transfer is expected to be smallest (probably close to zero) for the large and weakly coordinating anions when the anions and cations are well separated from each other (i.e., no or only a little orbital overlap occurs). In this case excess charges very close to the integer values of $+1\,e$ for the cation and $-1\,e$ for the anion are expected. Thus, the observed highest BE values of the ring signals for the large and weakly coordinating anions indicate a situation in which no charge transfer occurs. For the smaller, more basic and more coordinating anions, which are in closer vicinity to the imidazolium ring, the much more localised charge is transferred from the anion to the cation, leading to a less positively charged ring and in turn to lower XPS BEs. As a consequence of the overall charge neutrality, the negative excess charge of the anion must also deviate from the formal value of $-1\,e$ in the ILs. Hence, the small and strongly coordinating anions (such as the halides and $[NO_3]^-$) carry less negative charge compared to the large anions $[Tf_2N]^-$ and $[FAP]^-$. The degree of the ionic character of the ILs in a chemical meaning is thus affected by the choice of combination of anion and cation (the term "ionicity" will be avoided here because it is commonly used to describe transport properties and degree of association of anion and cation[25]). The saturation effect seen in Figure 4 for ions larger than $[BF_4]^-$ indicates that the charge transfer reaches values close to zero above a certain size of the weakly coordinating anions.

While in Figure 4a and 4b the molecular volume was chosen as an easily quantifiable parameter to correlate the amount of charge transfer between anion and cation, it is evident that specific interaction parameters, such as coordination characteristics of the molecules (e.g. shapes, terminal groups, etc.), will also play an important role. Accordingly, a much better correlation of the differential BE shift is found with the Kamlet–Taft parameter β (Figure 4c), as it is a measure of the hydrogen-bond acceptor ability of an IL's anion, which directly relates to the anion's coordination strength and charge localisation.[9,71] The dipolarity/polarisability parameter π^* also reflects the coordination ability of a given anion; however this value incorporates contributions from both the anion and cation as has been shown recently by Lungwitz et al.[71]

It should also be mentioned that counterion-dependent shifts of XPS core levels have been observed before in ionic crystals, but no clear statement on their origin has been made.[76–78] However, these data show similar trends to that observed in our study, that is, shifts of the respective cation core levels to higher BE for larger and less basic anions. Unfortunately, the question of reference level is not easy to handle for those earlier described inorganic salts in comparison to our well-adapted internal referencing method using the cation's octyl chains. Therefore, we refrain from a quantitative and detailed comparison of these previous studies on solid salts with our findings.

To corroborate our interpretation of the anion-dependent XPS shifts as a measure for the charge transfer between ions, detailed quantum chemical calculations on the representative ILs $[C_8C_1Im]X$ and $[C_8C_1C_1Im]X$ ($X = Cl^-$, Br^-,

$[BF_4]^-$, $[Tf_2N]^-$) in form of gas-phase ion pairs were performed. For the non-methylated $[C_8C_1Im]^+$ ILs, the in-plane configurations (i.e., the anion in-plane of the imidazolium ring in front of the C^2 position) were found to be energetically favoured. However, "on-top" configurations (i.e., the anion located above the ring plane in close proximity to the C^2–H^2 bond) were found to lie only at slightly higher energies and, thus, will also be considered here.[13,79] Especially for the larger and less-strongly coordinating $[Tf_2N]^-$ ion, the on-top configuration is energetically degenerate, that is, it has the same energy, or is even slightly favoured, with respect to the in-plane configuration. In case of the methylated $[C_8C_1C_1Im]^+$ ILs, only on-top configurations were found to be energetically stable. These low-energy conformers agree well with results from comparable imidazolium ion pair calculations.[8] It should be mentioned at this point that a detailed discussion on geometry and total energy of different conformers is beyond the scope of the present contribution and will be provided elsewhere. Here, we will restrict ourselves to the aspects directly related to our experimental findings.

In Table 2 the sums over partial charges for different moieties of $[C_8C_1Im]X$ and $[C_8C_1C_1Im]X$ ion pairs (X = Cl^-, Br^-, $[BF_4]^-$, $[Tf_2N]^-$) as well as the isolated $[C_8C_1Im]^+$ ion (labelled as "monomer" in Table 2) are given as derived by natural population analysis (NPA). It is evident that the overall excess charges of the cation and anion are non-integer and smaller than one in all cases except for the isolated $[C_8C_1Im]^+$ ion, for which the charge +1 e is imposed by boundary conditions. Thus, charge transfer between anion and cation is clearly indicated by the NPA. Most of the positive charge on the cation is located on the atoms of the ionic headgroup (labelled R′ in Table 2), in which it is nearly equally distributed over the imidazolium ring R and each of the two adjacent methyl (C^6) and methylene (C^7) groups bonded to the nitrogen atoms of the ring (note that R′ comprises the atoms C_{hetero} and N_{cation} measured in XPS). The two different in-plane and on-top conformers of the $[C_8C_1Im]X$ ILs show only minor deviations in charging of R′. Only for $[Tf_2N]^-$ is the difference somewhat larger, which could be related to the higher degree of flexibility of the $[Tf_2N]^-$ ion compared to the more spherical anions. The insensitivity of the excess charge to the different in-plane/on-top geometries is particularly surprising for the strongly coordinating Cl^- and Br^- ions, because of the different type of orbital interaction as it will be detailed in the next section. In short, for the in-plane configuration the charge transfer between the halide anion and the cation occurs mainly under strong participation of σ-type MOs of the cation located at the C^2 position and the p atomic orbitals of the anion (i.e., more hydrogen-bonding interactions), whereas for the on-top configuration anion and cation mainly interact through π orbitals of the imidazolium ring (i.e., more π-type bonding interactions). Nevertheless, both geometries with their individual charge-transfer mechanisms yield similar net charges of R′. These findings are in line with earlier results for $[C_4C_1Im]Cl$.[22] The relative distribution of the excess charge on the groups of the cation is similar for all anions and resembles the intrinsic charge distribution of the monomer (see Table 2). However, the absolute values of the NPA charges are significantly affected by the anion. Whereas the small, basic and strongly coordinating anions Cl^- and Br^- yield the smallest values for the charges on the ionic headgroup R′ (e.g., a mean value of 0.76 e in both configurations), the positive charge is considerably increased by +0.12 e for the larger, less basic and more weakly coordinating $[BF_4]^-$ and $[Tf_2N]^-$. The highest value for the positive charge on R′ of 0.91 e is found for $[Tf_2N]^-$ in the energetically favoured on-top configuration (coming close to the nominal value of one). Hence, the measured increase in XPS BEs of C_{hetero} and N_{cation} with increasing anion size and decreasing anion basicity is indeed directly reflected by an increase in positive charge on the ionic headgroup, as proposed above. To the best of our knowledge, this is the first time that interionic charge-transfer phenomena found for ILs in theory could be directly related to experimentally observable chemical shifts in XPS.

Table 2. NPA charge distribution in units of the elementary charge e summed over chemical groups for selected ion pairs.

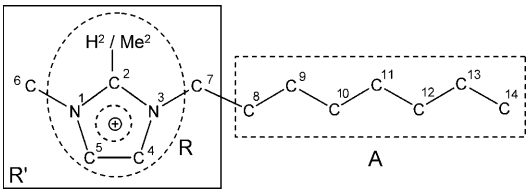

$[C_8C_1Im]^+$	Monomer	$[C_8C_1Im]X$ for in-plane/on-top configuration			
group/anion	–	$[Cl]^-$	$[Br]^-$	$[BF_4]^-$	$[Tf_2N]^-$
cation (=−anion)	1	0.811/0.791	0.824/0.803	0.940/0.964	0.936/0.972
ionic headgroup R′	0.920	0.762/0.742	0.772/0.751	0.860/0.906	0.850/0.913
imidazolium ring R	0.388	0.265/0.269	0.272/0.272	0.359/0.384	0.353/0.394
$(CH_3)^6$	0.293	0.263/0.260	0.266/0.263	0.291/0.285	0.286/0.281
$(CH_2)^7$	0.239	0.235/0.214	0.234/0.217	0.210/0.236	0.211/0.238
alkyl rest A	0.080	0.049/0.049	0.052/0.052	0.080/0.058	0.086/0.059
$[C_8C_1C_1Im]^+$	Monomer	$[C_8C_1C_1Im]X$ for on-top configuration			
group/anion	–	$[Cl]^-$	$[Br]^-$	$[BF_4]^-$	$[Tf_2N]^-$
cation (=−anion)	1	0.838	0.893	0.966	0.970
ionic headgroup R′	0.925	0.787	0.833	0.927	0.927
imidazolium ring R	0.311	0.258	0.292	0.320	0.306
$(CH_3)^6$	0.284	0.256	0.262	0.270	0.278
$(CH_2)^7$	0.233	0.209	0.207	0.246	0.250
Me^2	0.097	0.064	0.071	0.090	0.093
alkyl rest A	0.075	0.051	0.060	0.039	0.043

Moreover, the calculations clearly show that the anion-dependent charging of the ionic headgroup takes place independently of the methylation at C^2. In particular, the on-top configuration NPA charges on R′ of the non-methylated ILs $[C_8C_1Im]Br$ (0.75 e) and $[C_8C_1Im][Tf_2N]$ (0.91 e) ILs and their methylated counterparts $[C_8C_1C_1Im]Br$ (0.83 e) and $[C_8C_1C_1Im][Tf_2N]$ (0.93 e) reveal a common increase of at least +0.1 e of the ionic headgroup when the small and basic Br^- is replaced by the larger and less basic $[Tf_2N]^-$ ion. This is in very good agreement with the measured BE shifts of C_{hetero} and N_{cation} shown in Figure 5. As is also indicated in Table 2, the additional methyl group at C^2 of $[C_8C_1C_1Im]^+$ ILs carries a minor contribution (about 0.07 e, only weakly anion dependent) to the total positive charge of the ionic headgroup. The positive NPA charges of this methyl group are thus considerably smaller than the NPA charges on the N–$\mathbf{C}H_3$ and the N–$\mathbf{C}H_2$ carbon atoms, but larger than the NPA charges on methylene groups in the octyl chain (which are rather neutral, see Figure 1). This explains the intermediate C 1s peak position of the methyl group between the C_{hetero} and the C_{alkyl} position found by our XPS analysis (see Figure 5).

One should note that the different degree of charge transfer that is presumably responsible for the observed XPS shifts of the cationic headgroup is directly reflected by the degree of mixing of molecular orbitals between cation and anion. In Figure 6 the three highest occupied orbitals (HOMOs) and the lowest unoccupied MO (LUMO) of three ion pairs $[C_8C_1Im]Cl$, $[C_8C_1Im][BF_4]$ and $[C_8C_1Im][Tf_2N]$ in the low-energy in-plane configurations are shown. In case of the smallest and most basic Cl^- ion, a pronounced mixing of the Cl 2p atomic orbitals with molecular orbitals from the imidazolium cation is found. For the HOMO of the $[C_8C_1Im]Cl$ ion pair, which is dominated by the p states of Cl^-, and for the LUMO dominated by the cation, considerable density of states is present on the imidazolium ring and on the Cl^- ion as well. Mixing of orbitals becomes, however, more evident for the lower lying HOMO−1 and HOMO−2. In particular, the HOMO−2, which has a pronounced π-type bond character, exhibits strong interaction between the Cl 2p states and states localised at the -N^1-C^2H-N^3- unit of the imidazolium ring. As was stated earlier,[22] it is this HOMO−2 orbital that is important for the hydrogen-bond formation between the cation and the Cl^- ion. For the on-top configuration of $[C_8C_1Im]Cl$ the HOMO, HOMO−2 and HOMO−3 MOs show pronounced orbital mixing between the Cl 2p states and the cationic headgroup, evident in Figure 7. Upon replacement of Cl^- by the much larger and less basic $[BF_4]^-$ and $[Tf_2N]^-$ ions, no comparable strong mixing of orbitals could be detected for the in-plane configuration as it is shown in Figure 6. The character of MOs of the ion pairs for the in-plane configuration (Figure 6) is mainly given by either the MOs from the cation or MOs of the anion. As depicted in Figure 7 for the on-top configura-

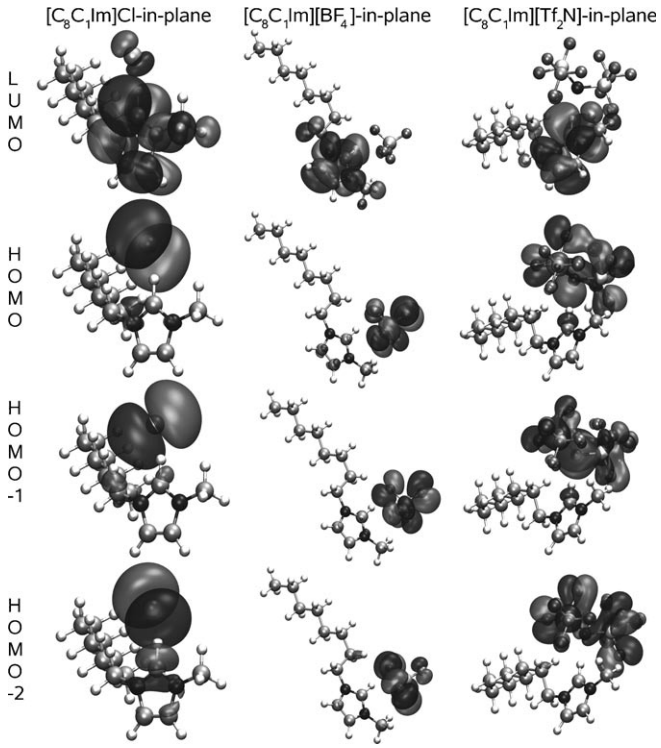

Figure 6. Frontier orbitals of $[C_8C_1Im]X$ ($X = Cl^-$, $[BF_4]^-$, $[Tf_2N]^-$) in in-plane configuration (isosurface value 0.02 for all orbitals).

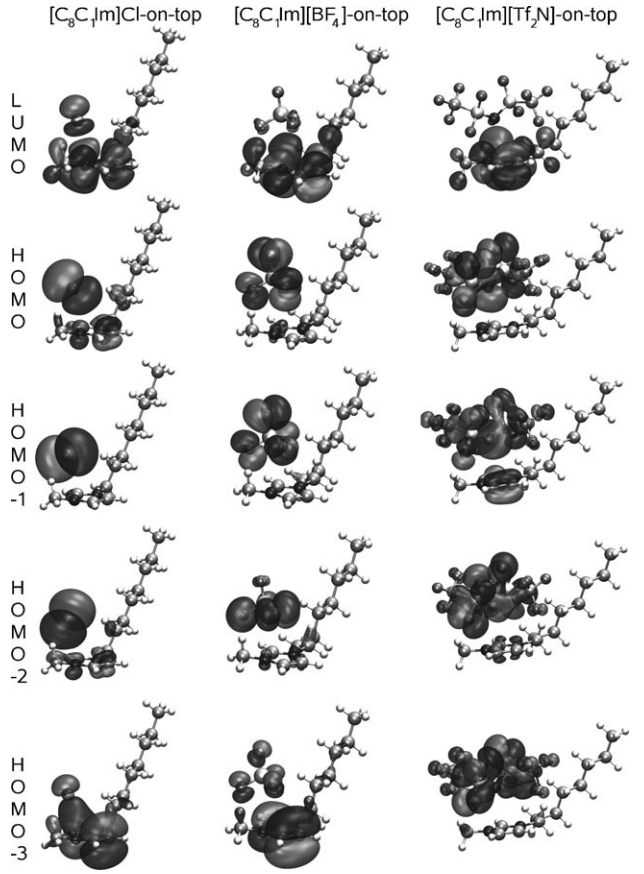

Figure 7. Molecular orbitals of $[C_8C_1Im]X$ ($X = Cl^-$, $[BF_4]^-$, $[Tf_2N]^-$) in on-top configuration (isosurface value 0.02 for all orbitals).

tion of $[C_8C_1Im][BF_4]$ and $[C_8C_1Im][Tf_2N]$, only some minor orbital mixing is observed in the HOMO−3 for $[C_8C_1Im][BF_4]$ and in the HOMO−1 of $[C_8C_1Im][Tf_2N]$, which accounts for the slightly reduced charges in these ILs. Furthermore, the frontier orbitals of $[C_8C_1C_1Im]Cl$ in on-top configuration were calculated and compared to the $[C_8C_1Im]Cl$ conformers from Figures 6 and 7 (see also Figure S3 in the Supporting Information). $[C_8C_1C_1Im]Cl$ on-top shows the same pronounced orbital mixing as it was discussed in the case of $[C_8C_1Im]Cl$ on-top, which further corroborates our interpretation of results.

As an intermediate summary, our XPS results in combination with quantum chemical calculations clearly indicate a strong electronic interaction between anion and cation for small, basic and strongly coordinating anions. This interaction leads to a partial charge transfer between anion and cation and, as a consequence, to effective charges considerably smaller than one. The amount of charge transfer decreases with increasing anion size and decreasing basicity, that is, with decreasing coordination strength. For the $[PF_6]^-$, $[TfO]^-$, $[Tf_2N]^-$, $[Pf_2N]^-$ and $[FAP]^-$ ions, which are all of low basicity and low coordination strengths, charge transfer is very small (<0.1 e) leading to values of the charges close to the ideal values ±1 e. We believe that these findings are crucial for the understanding of ionicity and polarity of ILs in general. Moreover, correct charges assigned in MD simulations are most important to obtain correct interaction potentials, especially for coulombic interactions.

As emphasised in the introduction, in addition to coulombic interactions also hydrogen-bonding-type interactions play an important role. Thus, in order to obtain complementary information on the molecular interactions between anion and cation and on the influence of these hydrogen bonds on electron density ^1H and ^{13}C NMR measurements on the ten $[C_8C_1Im]^+$-based ILs were carried out, and the results are compared to the XPS findings in the following.

^1H and ^{13}C NMR spectra of the $[C_8C_1Im]^+$-based ILs: To rule out any influence of solvents, ^1H and ^{13}C NMR spectra of the neat ILs were recorded. For all ILs, the spectra arising from the H^2, H^4 and H^5 protons and the corresponding C^2, C^4 and C^5 carbon atoms of the cation (labelled in Scheme 1) are shown in Figure 8a and 8c, respectively. Both the ^1H and ^{13}C NMR spectra show anion-dependent shifts.

^1H NMR of $[C_8C_1Im]X$ ILs: Focusing first on the ^1H NMR signals of the imidazolium ring in Figure 8a, all peaks shift towards lower ppm values when going from small, basic and strongly coordinating anions to larger, less basic and weaker coordinating anions. Our data agree very well with previously published ^1H NMR data by Tokuda et al., who investigated neat $[C_4C_1Im]^+$ salts carrying $[TfO]^-$, $[Tf_2N]^-$, $[Pf_2N]^-$, $[BF_4]^-$ and $[PF_6]^-$ counterions.[11] The NMR shift is largest for the H^2 proton (from 9.9 ppm for Cl^- to 7.4 ppm for $[FAP]^-$) and slightly smaller for the H^4/H^5 signals (from 7.9 ppm for Cl^- to 6.5 ppm for $[FAP]^-$). The correlation of the NMR shifts with the size of the anion is shown in Figure 8b, in which ^1H NMR positions of the ring protons are plotted against IL molecular volume. The data reveal a similar overall trend as the chemical shifts in XPS (Figure 4): with increasing molecular volume, a steep decrease in ppm shifts from Cl^- to about $[BF_4]^-/[PF_6]^-$ is measured, followed by a plateau-type behaviour for the larger anions (dashed

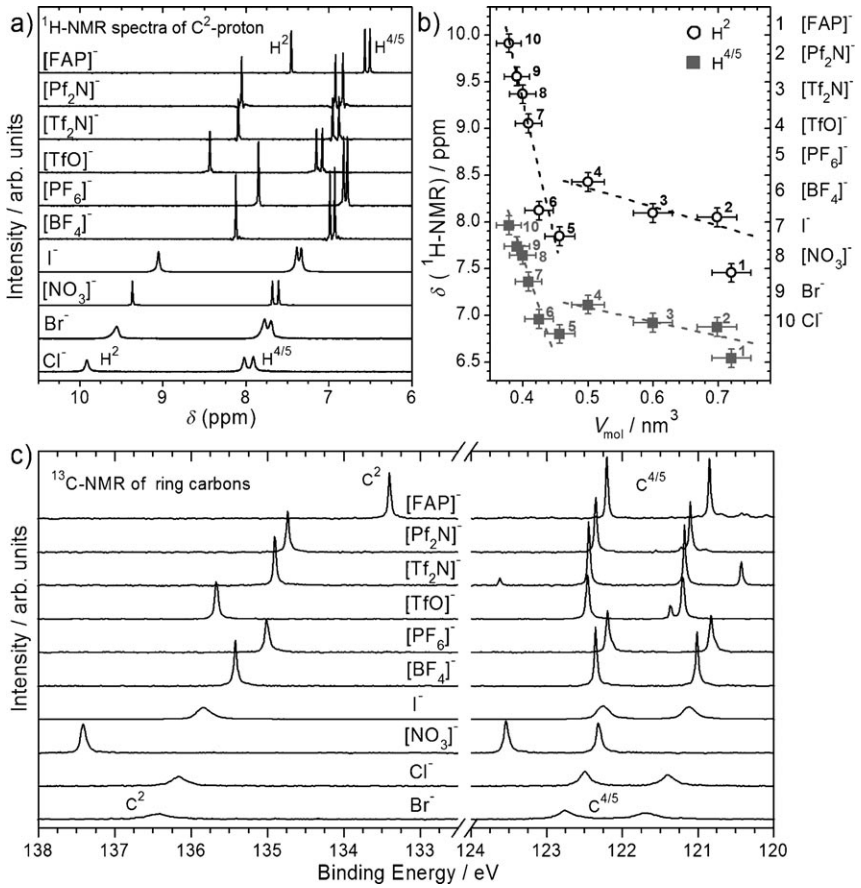

Figure 8. a) ^1H NMR spectra of H^2 and $H^{4/5}$ of $[C_8C_1Im][X]$. b) Correlation of ^1H NMR resonances of H^2 (open circles) and $H^{4/5}$ (solid squares, values are for mid position for H^4/H^5) with molecular volume (dashed lines are guide to the eye). c) ^{13}C NMR spectra of C^2 and $C^{4/5}$ of $[C_8C_1Im][X]$; the spectra are offset for sake of clarity in the order of increasing molecular volume.

lines in Figure 8b). Again, it should be mentioned that anion size is a rough, but easily accessible parameter that seems to give a good correlation as long as spherical anions (with a spherical charge distribution) are considered. Also, a very good overall correlation can be found when correlating the NMR shifts with the ILs' Kamlet–Taft parameters[9] α and β, which represent the hydrogen-bond donor and acceptor capability of the IL, respectively (see Figure S4 in the Supporting Information).

Such anion-dependent ^{1}H NMR shifts have been commonly interpreted as a measure for the extent of hydrogen bonding in imidazolium-based ILs or as a measure of the extent of π stacking of the imidazolium rings.[28,29,73,80] As the imidazolium cation is surrounded by anions, the ^{1}H NMR shift of H^2, H^4 and H^5 is a result of an equilibrium of several ion-pair structures.[81] Increased π stacking—as predicted for an increasing concentration of ILs diluted in common solvents—generally leads to a shift towards lower ppm values.[28] In our case of pure ILs it appears unlikely that the very large and weakly coordinating $[Pf_2N]^-$ and $[FAP]^-$ ions yield a higher degree of association to the imidazolium cations and, thus, a better π stacking than the small halides. Lungwitz and Spange observed an analogous anion-dependent H^2 shift for a series of $[C_4C_1Im]^+$-based ILs, with the ILs sufficiently diluted in CD_2Cl_2 to ensure that they are mainly present as ion pairs. The measured NMR shifts were unambiguously identified as a measure for hydrogen-bonding-type interactions between the anion and the cation, because of their good correlation with corresponding Kamlet–Taft parameters α and β of the ILs as probed by solvatochromic dyes.[9,10] According to the interpretation of the Spange group, the interaction with small and strongly coordinating anions leads to a weakening of the C^2–H^2 bond, and thus, to a proton resonance closer to that of an acidic proton. Comparing the data from Lungwitz with our measurements, the trend of the ^{1}H NMR signals of the H^2 proton with the different anions is similar; however, in our case of the pure ILs absolute values for the ppm positions are about 0.5 ppm smaller, which is attributed to the influence of the solvent. Hence, we adapt the interpretation for our observed anion-dependent ^{1}H NMR shifts, which are primarily attributed to changes in the magnetic shielding constant at the H^2 and (to a lesser extent) the H^4 and H^5 protons. Shifts towards higher ppm and, thus, less pronounced shielding of the protons, indicate stronger hydrogen bonding and vice versa. This is in line with the qualitative picture of diamagnetic shielding in NMR: the lower the electron density at the place of the ^{1}H nucleus (as it is the case of pronounced hydrogen bonding), the weaker the local shielding of the external magnetic field leading to higher ppm shifts. (It is important to note that quantification of NMR shifts is very complicated—particularly in case of delocalised π-electron systems—and many theoretical approaches have been employed in the past to ascribe for the different effects.[82]) As the concentration of the ILs is not varied in our case and the structure of the $[C_8C_1Im]^+$ ion remains virtually unchanged in our series, we do not expect that variations in π stacking have a strong influence on the observed ^{1}H shifts. Nevertheless, it is interesting to note that $[C_8C_1Im][BF_4]$ and $[C_8C_1Im][PF_6]$ are to some extent outliers in the series exhibiting smaller shifts than expected from their molecular volume (see Figure 8b), which might be attributed to the fact that for these anions very low basicity and coordination strength is combined with relatively small molecular volume compared to the larger fluorinated anions in this study.

^{13}C NMR of $[C_8C_1Im]X$ ILs: In the hydrogen-bonding scheme described above, smaller, more basic and stronger coordinating anions lead to a more pronounced loss in electron density at the position of the ring protons and consequently to high ppm shifts in the ^{1}H NMR spectra. Thus, one might expect that the neighbouring carbon atoms C^2, C^4 and C^5 simultaneously gain in electron density. This assumption is supported by the anion-dependent C 1s and N 1s XPS shifts of the imidazolium ring, which indicate an increase in electron density within the ring for the small anions as compared to the large, less basic and weakly coordinating anions. As a consequence, the ^{13}C NMR signals of the ring carbon atoms should shift towards LOWER ppm with decreasing size of the anion, due to a higher shielding within the imidazolium ring if the electron density were the sole contribution to the signal shifts (see also the discussion on charge density and ^{13}C NMR for typical aromatic compounds given by Wiberg et al.[83]). In Figure 8c the ^{13}C NMR data of the ring carbon atoms of all $[C_8C_1Im]^+$ ILs are shown. Overall, the ^{13}C NMR signals of the imidazolium ring are approximately constant within the whole series and changes are very small. The differential shifts of the C^2 signal amounts to ±1.5 ppm around 135 ppm, and those of the C^4/C^5 signals to ±0.5 ppm around 122.5 ppm, being therefore in the range of typical heteroaromatic compounds, and are more or less independent of the anion (only $[C_8C_1Im][NO_3]$ seems to be an outlier with larger shifts of the ring carbon atoms). Hence, ^{13}C NMR seems to be rather insensitive to the influence of the anion. However, a weak trend is observed: for smaller, more basic and more strongly coordinating anions the ^{13}C NMR signals slightly shifts towards higher ppm (most pronounced at C^2). Hence, ^{1}H and ^{13}C NMR signals exhibit "parallel" shifts for the C^2–H^2 group of the ring, as seen in Figure 8c, which contradicts the simple consideration of electron densities. It seems that some compensating effects are present, such as changes in the ring current, hybridisation re-arrangements accompanied with anisotropy changes and so forth, which are known to have an impact on local shielding effects in ^{13}C NMR. In particular, it has been shown for monocyclic aromatic compounds that it is the degree of p_z occupancy for sp^2-hybridised ring carbon atoms rather than the local charge density that affects the ^{13}C NMR shifts.[83] Therefore, we assume that the different degree of orbital mixing (see also Figure 6 and the discussion in the preceding chapter) has a direct impact on the ^{13}C NMR shifts, as well as the more straightforward charge-density considerations.

If this assumption was correct one should expect anion-dependent changes in hybridisation of the imidazolium ring. For that reason we performed a NBO analysis of selective bonds within the imidazolium ring using natural resonance theory (NRT).[64] Here, NBO values of 1 and 2 describe classical single and double bonds, respectively, whereas values close to 1.5 in the aromatic compound benzene would correspond to a classical aromatic bond. Since the effect of the different anions on the NBO values is rather small, we compare the isolated $[C_8C_1Im]^+$ ion (representing the most extreme case, in which an coordinating anion is absent) with $[C_8C_1Im]Cl$ (NBO averaged for in-plane and on-top configuration) as the other extreme case of the most strongly coordinating anion of our study.

From Figure 9, in the case of the weakly coordinating anion (i.e., the isolated cation), the ring bonds exhibit a pronounced aromatic bond character with a delocalised π

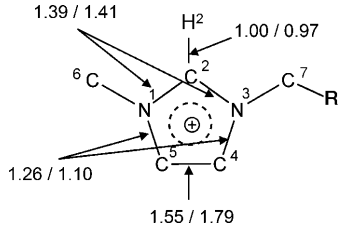

Figure 9. NBO values from NRT of selected ring bonds in the isolated $[C_8C_1Im]^+$ ion (first value) and in the $[C_8C_1Im]Cl$ ion pair (second value, average of in-plane and on-top configuration).

system (NBOs varies from 1.39 for the N^1-C^2-N^3 bonds, 1.26 for the N^1-C^5/N^3-C^4 bonds to 1.55 for the C^4-C^5 bond). For the strongly coordinated $[C_8C_1Im]Cl$ ion pair, the ring bonds resemble more an Arduengo carbene with a double bond at C^4-C^5 (1.79), whereas the N^1-C^5/N^3-C^4 bonds exhibit single-bond character (1.10). The reduced NBO value for the C^2–H^2– bond (0.97, 0.94 for the in-plane-configuration) is a clear indication for the hydrogen bonding of the H^2 proton with the coordinating Cl^- ion, as already discussed in the context of the ^{1}H NMR data; see also reference [22]. An illustration of the proposed interactions and changes in hybridisation (representative for the in-plane configurations) is given in Scheme 2, in which both the degree of hydrogen bonding as well as slight changes in hybridisation and aromaticity of the system are depicted. This interaction scheme is also supported by the work of Fumino et al.,[12,14] who find a significant weakening in the C^2–H^2 vibrational bands for the more strongly coordinating anion $[NO_3]^-$ as compared to $[BF_4]^-$.

Our interpretation is supported by the ^{13}C NMR chemical shifts for the classical imidazolium compound $[C_1C_1Im]Cl$ (C^2 resonance at 135 ppm) and the corresponding extreme case of complete proton abstraction, an Arduengo carbene (C^2 resonance at 213.7 ppm).[84] In case of the carbene, changes in hybridisation, and thus, changes in shielding con-

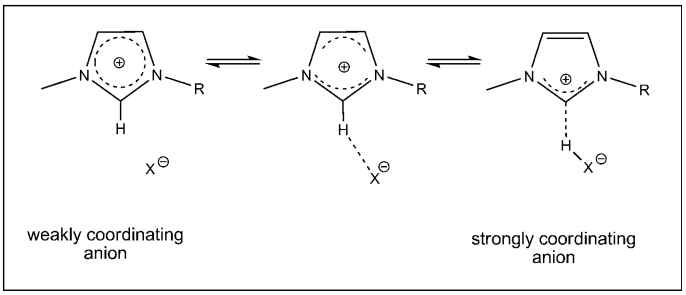

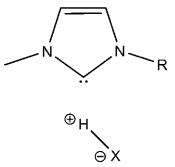

extreme case of complete proton abstraction: Arduengo carbene

Scheme 2. Interaction scheme of the imidazolium ring with a given anion.

stant, lead to a strong increase in chemical shift despite the fact that the electron density at the place of the C^2-position is evidently enhanced. Although our results from the NBO analysis point in the right direction, further theoretical investigations would be very helpful to elucidate details in electronic structure of the ring of the cation as a function of the anion, especially for the larger, less basic and very weakly coordinating ones.

NMR results from $[C_8C_1C_1Im][X]$ ILs: To consolidate our interpretation of ^{1}H and ^{13}C NMR shifts of $[C_8C_1Im][X]$ ILs, a comparison was made with the C^2-methylated ILs $[C_8C_1C_1Im]Br$ and $[C_8C_1C_1Im][Tf_2N]$. As $[C_8C_1C_1Im]Br$ is solid at room temperature, a liquid 5:1 mixture of $[C_8C_1Im]Br$:$[C_8C_1C_1Im]Br$ was investigated. ^{1}H and ^{13}C NMR spectra of the respective ILs are shown in Figure 10.

From the ^{13}C NMR measurements it can clearly be seen that the peak assigned to C^2 undergoes a clear downfield shift of about 8 ppm towards higher values upon methylation, which is a general feature in aromatic systems, when a proton is substituted with a methyl group.[85] This shift is commonly assigned to a change in electron current at the ^{13}C nucleus resulting from the different bonding environment (exchange of s-type(H) with sp^3-type(C) orbital). In contrast, the $C^{4/5}$ signals undergo a highfield shift of $\approx$1.5 ppm, which could be assigned to the molecular changes due to methylation. However, this shift can also be related to the slight highfield shifts observed for the $H^{4/5}$ protons in ^{1}H NMR. While in the spectra of $[C_8C_1C_1Im]Br$ and $[C_8C_1C_1Im][Tf_2N]$ no H^2 peak is present, the $H^{4/5}$ peaks are subject to a subtle highfield shift of about 0.2 ppm for both ILs, which indicates less pronounced (or at least no enhanced) hydrogen bonding through $H^{4/5}$. This means that upon methylation of the C^2 position the main hydrogen-

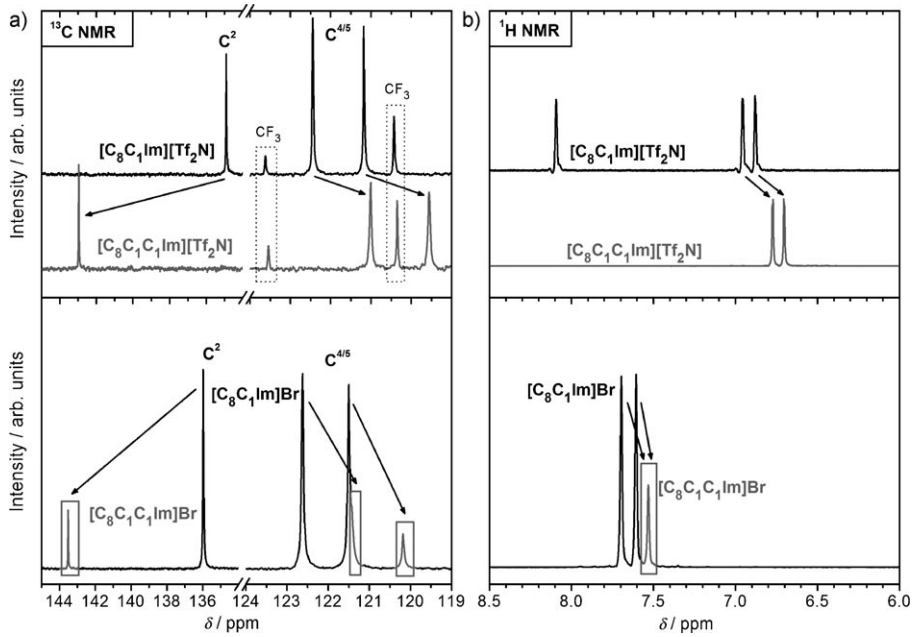

Figure 10. Imidazolium ring signals in a) ^{13}C and b) ^{1}H NMR of $[C_8C_1Im][Tf_2N]$ (black curves) and $[C_8C_1C_1Im][Tf_2N]$ (grey curves) (top row) and of the 5:1 mixture of $[C_8C_1Im]Br$:$[C_8C_1C_1Im]Br$ (black curve, bottom) are compared (signals originating from the $[Tf_2N]^-$ ion in this region are indicated by boxes). The differential ppm shifts due to methylation at C^2 are marked by arrows.

bonding interaction is indeed eliminated and to no extent compensated by the $H^{4/5}$ protons.

Concluding our results from NMR and the NBO analysis, the interaction between anions and the imidazolium cations through hydrogen-bonding-type interactions is strongly altered by the nature of the anion. Small and more basic anions exhibit pronounced hydrogen bonding with the hydrogen atoms of the ring (particularly with H^2) as compared to the larger and less basic anions. Moreover, the electronic structure of the imidazolium ring in terms of charge distribution is modified by the coordination ability of the anion—large and weakly coordinating anions lead to a more aromatic character of the π system of the ring; this is in contrast to the case of small, more basic and, thus, more strongly coordinated anions, which yield a more carbene-like charge distribution in the ring. Importantly, we find no evidence that the presence or absence of intermolecular hydrogen bonds considerably influences the absolute value of the net charge transfer between anion and cation; this is deduced from our XPS results and DFT calculations in combination with our NMR data for the methylated and non-methylated ILs.

Conclusion

In this systematic XPS, NMR and theoretical study ten $[C_8C_1Im]^+$- and two $[C_8C_1C_1Im]^+$-based ILs were investigated. In XPS, we find an anion-dependent shift of the C 1s and N 1s levels originating from the headgroup of the imidazolium cation towards higher BE for larger, less basic and, thus, less coordinating anions. This shift is interpreted as a measure for the net positive charge on the imidazolium ring with the adjacent methyl and methylene groups. The charge transfer between anion and cation is unambiguously related to the nature of the anion: for spherical anions a linear correlation of the BE shift with IL molecular volume is observed, whereas for the more asymmetric large anions carrying perfluoralkyl groups, the BE shift exhibits only minor changes with increasing size. Overall, a linear correlation with the hydrogen-bond acceptor basicity of the anion—characterised by the corresponding Kamlet–Taft parameter β—is found, which indicates that the interionic charge transfer is closely related to the anion's coordination strength and, thus, to the localisation of the negative excess charge in the anion. These findings are corroborated by DFT calculations on isolated $[C_8C_1Im]X$ ion pairs, which show that a net charge transfer through orbital mixing of anion and cation occurs for all energetically favourable conformations (i.e., the, "on-top" and "in-plane" configurations). The positive excess charge on the ionic headgroup of the cation varies from $+0.75\,e$ for $[C_8C_1Im]Cl$ up to of $+0.91\,e$ for $[C_8C_1Im][Tf_2N]$, coming close to the nominal value $+1.0\,e$. Our calculations also show that for less basic, less strongly coordinating anions, the on-top configuration is energetically favoured; this also holds true for the homologue ILs $[C_8C_1C_1Im]X$, in which the most acidic proton in the 2-position is substituted by a neutral methyl group. Despite the considerably lower contribution of hydrogen-bond-type interactions in the methylated $[C_8C_1C_1Im]X$ ILs (deduced from natural bond order (NBO) analysis and ^{1}H NMR spectroscopy), the anion-dependent charge transfer is nearly identical to that for the non-methylated homologue ILs (deduced by natural population analysis of atomic charges (NPA) and XPS). Thus, the anion-dependent charge transfer cannot solely be mediated through pronounced hydrogen bonding, but is most likely dominated by the degree of orbital mixing of anion and cation. This contribution is strongly depending on the proximity of the ions; hence, the local charge distributions play a crucial role.

Apart from coulombic interactions related to the charged ions, the understanding of the role of hydrogen-bonding-type interactions is essential for ILs. The analysis of the ^{1}H NMR spectra of pure ILs, in which additional solvent in-

teractions can be ruled out, reveals that the increasing size of the anion, accompanied by gradual reduction in anion basicity, leads to a reduction in hydrogen bonding, which is in line with findings from other groups measuring ILs in organic solvents. The ^{13}C NMR signals of the imidazolium ring are only weakly influenced by the nature of the anion. However, a small shift of the signal from the carbon atom in the 2-position reflects an anion-dependent change of electronic structure within the ring, which is likely related to alterations in ring hybridisation, an argument that is also supported by our NBO analysis. Hence ^{1}H NMR reflects very well the influence of different anions on the ion pair interactions by hydrogen bonding, whereas ^{13}C NMR is less sensitive to hydrogen-bonding interactions.

We are confident that an approach towards a detailed understanding of intermolecular interactions in ionic liquids as reported in this communication can be extended to other liquid systems, where these types of interactions also play an important role. This understanding will also provide a better interpretation of parameters (e.g., effective charges) commonly used in molecular dynamics.

Experimental Section

Ionic liquids: An overview of all ILs studied in this work is given in Table 1. $[C_8C_1Im][FAP]$, $[C_8C_1C_1Im][Tf_2N]$ and $[C_8C_1C_1Im]Br$ were kindly given by Merck, while $[C_8C_1Im]I$ and $[C_8C_1Im][NO_3]$ were provided by Alasdair Taylor from the Licence group at University of Nottingham and Ralf Lungwitz from the Spange group at University of Chemnitz, respectively. $[C_8C_1Im][Tf_2N]$, $[C_8C_1Im][Pf_2N]$ and $[C_8C_1Im]Cl$ were synthesised under ultra-clean conditions in our laboratories. $[C_8C_1Im]Br$ and $[C_8C_1Im][PF_6]$ were purchased from Merck, $[C_8C_1Im][BF_4]$ and $[C_8C_1Im][TfO]$ from Sigma–Aldrich.

XPS measurements: Thin IL films (thickness ≈ 0.2 mm) were prepared by deposition of the corresponding IL onto a planar, pre-cleaned Au foil. In the load lock chamber of the XPS apparatus the IL samples were carefully degassed at a pressure of 1×10^{-6} mbar for at least 6 h to remove residual water and other possible volatile impurities.[43,54] XP spectra were taken with a VG ESCALAB 200 spectrometer with non-monochromatised $Al_{K\alpha}$ radiation ($h\nu = 1486.6$ eV). All spectra were recorded at a pass energy of 20 eV, resulting in an overall resolution of ≈ 0.9 eV, and at normal emission (0° with respect to the surface normal). Due to the inelastic mean free path of about 3 nm of photoelectrons in organic compounds[55] at the kinetic energies used (800–1300 eV), measurements at 0° average over several ion layers of the near-surface region (information depth, ID: 7–9 nm, depending on the kinetic energy). Hence, the measured BEs represent the electronic states of the corresponding ions in the bulk of the IL. The spectra were fitted using Gaussian functions after linear background subtraction. C 1s spectra were fitted individually with the constraint of full width at half-maximum, $FWHM(C_{hetero}) = 1.11 \times FWHM(C_{alkyl})$, in accordance with previously published results.[46,50,51] To allow for comparison of relative BE positions of different ILs, all spectra were shifted, such that the peak position of the seven aliphatic carbon species (C_{alkyl}) was at 285.0 eV (see also Results and Discussion section). This procedure was necessary to account for slight charging phenomena (± 0.15 eV), which have been observed and discussed before.[39] The unshifted C 1s spectra are shown in Figure S1 in the Supporting Information.

NMR measurements: ^{1}H and ^{13}C NMR measurements were performed using a JEOL ECX 400 MHz spectrometer. The ILs were carefully degassed at 10^{-3} mbar and then introduced into a standard NMR tube with a $[D_6]$DMSO-inset as external standard and reference. All spectra were recorded without additional solvent making this set of data a valuable NMR reference for a large set of pure $[C_8C_1Im]$-based ILs. Chemical shifts were referenced to DMSO with 2.50 and 39.51 ppm for ^{1}H and ^{13}C spectra, respectively.[56] For the measurement of the methylated IL $[C_8C_1C_1Im]Br$, which is a solid at room temperature, a liquid 5:1 mixture of $[C_8C_1Im]Br$ and $[C_8C_1C_1Im]Br$ was measured.

Computational methods: The models used in the present work are isolated ion pairs in the gas-phase. For all compounds, methods and basis sets applied the structures were always optimised. In most cases, more than one geometrical configuration of the anion relative to the cation was considered. All calculations from the Kirchner group were performed with the TURBOMOLE 5.10 program package[57] using density functional theory in combination with the dispersion corrected BLYP[58,59]-D[60] functional. This choice of functional and dispersion correction turned out to perform very well for ionic liquid ion pairs.[61,62] The TZVPP basis set was employed as implemented in the TURBOMOLE 5.10 program package; all calculations were combined with the resolution of identity technique calculations.[57] To obtain atomic charges, a natural population analysis (NPA) was carried out with the aid of the TURBOMOLE 5.10 implementation.[63] In order to avoid ambiguities in charge assignment to individual atoms, a sum of charges over characteristic groups of the molecules (e.g., CH_2 and CH_3 groups) is given. Orbitals were calculated with the TURBOMOLE 5.10 program package. The isosurface value for all orbitals was set to 0.02. The GAUSSIAN 03 program was employed for the NBO analysis under application of the TZVP basis set.[64,65] The NBO analysis was carried out employing the BLYP functional without the resolution of identity approximation. For comparison, ion-pair calculations independently performed in the Wasserscheid group for $[C_2C_1Im]X$ ILs (with $X = Cl^-$, $[BF_4]^-$, $[Tf_2N]^-$) with GAUSSIAN 03 using the B3LYP functional and the 6–311G basis set (for details, see reference [66]) reveal good agreement with the analogue calculations from the Kirchner group. Deviations in absolute values for the atomic charges between both types of calculation are considerably smaller than 10%; relative trends for the three different anions fully agree.

Acknowledgements

The authors like to thank the German Science Foundation (DFG) for financial support in the framework of its priority program 1191 "Ionic Liquids" (www.dfg-spp1191.de: STE 629/7-1 and 7-2, WA 1615/8-1 and 8-2, KI-768/5-1, and KI-768/5-2 as well as KI-768/4-1, KI-768/4-2 from the ERA chemistry). Furthermore, the authors thank the groups of Spange and Licence and Merck KGaA for providing selected IL samples and the Spange group for providing unpublished β parameters for $[C_8C_1Im]Cl$, $[C_8C_1Im]Br$ and $[C_8C_1Im][FAP]$. Additional support by the Erlangen Cluster of Excellence "Engineering of Advanced Materials" (www.eam.uni-erlangen.de) and computer time from the RZ Leipzig and NIC Jülich are also gratefully acknowledged.

[1] P. Wasserscheid, T. Welton, *Ionic liquids in synthesis*, 2nd ed., Wiley-VCH, Weinheim, **2008**.
[2] N. V. Plechkova, K. R. Seddon, *Chem. Soc. Rev.* **2008**, *37*, 123.
[3] I. Krossing, J. M. Slattery, C. Daguenet, P. J. Dyson, A. Oleinikova, H. Weingartner, *J. Am. Chem. Soc.* **2006**, *128*, 13427.
[4] U. P. R. M. Preiss, J. M. Slattery, I. Krossing, *Ind. Eng. Chem. Res.* **2009**, *48*, 2290.
[5] S. Zahn, F. Uhlig, J. Thar, C. Spickermann, B. Kirchner, *Angew. Chem.* **2008**, *120*, 3695; *Angew. Chem. Int. Ed.* **2008**, *47*, 3639.
[6] J. Thar, M. Brehm, A. P. Seitsonen, B. Kirchner, *J. Phys. Chem. B* **2009**, *113*, 15129.
[7] P. A. Hunt, *J. Phys. Chem. B* **2007**, *111*, 4844.
[8] P. A. Hunt, I. R. Gould, B. Kirchner, *Aust. J. Chem.* **2007**, *60*, 9.
[9] R. Lungwitz, M. Friedrich, W. Linert, S. Spange, *New J. Chem.* **2008**, *32*, 1493.
[10] R. Lungwitz, S. Spange, *New J. Chem.* **2008**, *32*, 392.

[11] H. Tokuda, S. Tsuzuki, M. Susan, K. Hayamizu, M. Watanabe, *J. Phys. Chem. B* **2006**, *110*, 19593.
[12] K. Fumino, A. Wulf, R. Ludwig, *Angew. Chem.* **2008**, *120*, 8859; *Angew. Chem. Int. Ed.* **2008**, *47*, 8731.
[13] S. Zahn, G. Bruns, J. Thar, B. Kirchner, *Phys. Chem. Chem. Phys.* **2008**, *10*, 6921.
[14] K. Fumino, A. Wulf, R. Ludwig, *Phys. Chem. Chem. Phys.* **2009**, *11*, 8790.
[15] J. N. Canongia Lopes, A. A. H. Padua, *J. Phys. Chem. B* **2006**, *110*, 19586.
[16] J. N. Canongia Lopes, J. Deschamps, A. A. H. Padua, *J. Phys. Chem. B* **2004**, *108*, 2038.
[17] T. Köddermann, D. Paschek, R. Ludwig, *ChemPhysChem* **2007**, *8*, 2464.
[18] B. L. Bhargava, S. Balasubramanian, *J. Chem. Phys.* **2007**, *127*, 114510.
[19] T. I. Morrow, E. J. Maginn, *J. Phys. Chem. B* **2002**, *106*, 12807.
[20] E. J. Maginn, *J. Phys. Condens. Matter* **2009**, *21*, 373101.
[21] T. G. A. Youngs, C. Hardacre, *ChemPhysChem* **2008**, *9*, 1548.
[22] P. A. Hunt, B. Kirchner, T. Welton, *Chem. Eur. J.* **2006**, *12*, 6762.
[23] H. Boroudjerdi, Y. W. Kim, A. Naji, R. R. Netz, X. Schlagberger, A. Serr, *Phys. Rep.* **2005**, *416*, 129.
[24] H. Tokuda, K. Hayamizu, K. Ishii, M. Susan, M. Watanabe, *J. Phys. Chem. B* **2005**, *109*, 6103.
[25] D. R. MacFarlane, M. Forsyth, E. I. Izgorodina, A. P. Abbott, G. Annat, K. Fraser, *Phys. Chem. Chem. Phys.* **2009**, *11*, 4962.
[26] V. Kempter, B. Kirchner, *J. Mol. Struct.* **2010**, *972*, 22.
[27] A. Elaiwi, P. B. Hitchcock, K. R. Seddon, N. Srinivasan, Y. M. Tan, T. Welton, J. A. Zora, *J. Chem. Soc. Dalton Trans.* **1995**, 3467.
[28] A. G. Avent, P. A. Chaloner, M. P. Day, K. R. Seddon, T. Welton, *J. Chem. Soc. Dalton Trans.* **1994**, 3405.
[29] D. Bankmann, R. Giernoth, *Prog. Nucl. Magn. Reson. Spectrosc.* **2007**, *51*, 63.
[30] J. Palomar, V. R. Ferro, M. A. Gilarranz, J. J. Rodriguez, *J. Phys. Chem. B* **2007**, *111*, 168.
[31] R. Giernoth, D. Bankmann, N. Schlorer, *Green Chem.* **2005**, *7*, 279.
[32] D. H. Zaitsau, G. J. Kabo, A. A. Strechan, Y. U. Paulechka, A. Tschersich, S. P. Verevkin, A. Heintz, *J. Phys. Chem. A* **2006**, *110*, 7303.
[33] J. P. Armstrong, C. Hurst, R. G. Jones, P. Licence, K. R. J. Lovelock, C. J. Satterley, I. J. Villar-Garcia, *Phys. Chem. Chem. Phys.* **2007**, *9*, 982.
[34] J. P. Leal, J. Esperanca, M. E. M. da Piedade, J. N. C. Lopes, L. P. N. Rebelo, K. R. Seddon, *J. Phys. Chem. A* **2007**, *111*, 6176.
[35] S. Krischok, M. Eremtchenko, M. Himmerlich, P. Lorenz, J. Uhlig, A. Neumann, R. Ottking, W. J. D. Beenken, O. Hofft, S. Bahr, V. Kempter, J. A. Schaefer, *J. Phys. Chem. B* **2007**, *111*, 4801.
[36] T. Nishi, T. Iwahashi, H. Yamane, Y. Ouchi, K. Kanai, K. Seki, *Chem. Phys. Lett.* **2008**, *455*, 213.
[37] O. Höfft, S. Bahr, M. Himmerlich, S. Krischok, J. A. Schaefer, V. Kempter, *Langmuir* **2006**, *22*, 7120.
[38] E. F. Smith, I. J. Villar Garcia, D. Briggs, P. Licence, *Chem. Commun.* **2005**, 5633.
[39] E. F. Smith, F. J. M. Rutten, I. J. Villar-Garcia, D. Briggs, P. Licence, *Langmuir* **2006**, *22*, 9386.
[40] D. S. Silvester, T. L. Broder, L. Aldous, C. Hardacre, A. Crossley, R. G. Compton, *Analyst* **2007**, *132*, 196.
[41] V. Lockett, R. Sedev, C. Bassell, J. Ralston, *Phys. Chem. Chem. Phys.* **2008**, *10*, 1330.
[42] J. M. Gottfried, F. Maier, J. Rossa, D. Gerhard, P. S. Schulz, P. Wasserscheid, H. P. Steinrück, *Z. Phys. Chem.* **2006**, *220*, 1439.
[43] C. Kolbeck, M. Killian, F. Maier, N. Paape, P. Wasserscheid, H. P. Steinrück, *Langmuir* **2008**, *24*, 9500.
[44] T. Cremer, M. Killian, J. M. Gottfried, N. Paape, P. Wasserscheid, F. Maier, H. P. Steinrück, *ChemPhysChem* **2008**, *9*, 2185.
[45] S. Caporali, U. Bardi, A. Lavacchi, *J. Electron Spectrosc. Relat. Phenom.* **2006**, *151*, 4.
[46] K. R. J. Lovelock, C. Kolbeck, T. Cremer, N. Paape, P. S. Schulz, P. Wasserscheid, F. Maier, H. P. Steinrück, *J. Phys. Chem. B* **2009**, *113*, 2854.
[47] Q. H. Zhang, S. M. Liu, Z. P. Li, J. Li, Z. J. Chen, R. F. Wang, L. J. Lu, Y. Q. Deng, *Chem. Eur. J.* **2009**, *15*, 765.
[48] N. Paape, W. Wei, A. Bosmann, C. Kolbeck, F. Maier, H. P. Steinrück, P. Wasserscheid, P. S. Schulz, *Chem. Commun.* **2008**, 3867.
[49] I. Lindgren, *J. Electron Spectrosc. Relat. Phenom.* **2004**, *137*, 59.
[50] C. Kolbeck, T. Cremer, K. R. J. Lovelock, N. Paape, P. S. Schulz, P. Wasserscheid, F. Maier, H.-P. Steinrück, *J. Phys. Chem. B* **2009**, *113*, 8682.
[51] F. Maier, T. Cremer, C. Kolbeck, K. R. J. Lovelock, N. Paape, P. S. Schulz, P. Wasserscheid, H.-P. Steinrück, *Phys. Chem. Chem. Phys.* **2010**, *12*, 1905.
[52] F. Maier, J. M. Gottfried, J. Rossa, D. Gerhard, P. S. Schulz, W. Schwieger, P. Wasserscheid, H. P. Steinrück, *Angew. Chem.* **2006**, *118*, 7942; *Angew. Chem. Int. Ed.* **2006**, *45*, 7778.
[53] S. Krischok, R. Ottking, W. J. D. Beenken, M. Himmerlich, P. Lorenz, O. Hofft, S. Bahr, V. Kempter, J. A. Schaefer, *Z. Phys. Chem.* **2006**, *220*, 1407.
[54] A. W. Taylor, K. R. J. Lovelock, A. Deyko, P. Licence, R. G. Jones, *Phys. Chem. Chem. Phys.* **2010**, *12*, 1772.
[55] R. F. Roberts, D. L. Allara, C. A. Pryde, D. N. E. Buchanan, N. D. Hobbins, *Surf. Interface Anal.* **1980**, *2*, 5.
[56] Bruker-Almanac, Bruker BioSpin, **2009** (http://www.bruker.com).
[57] R. Ahlrichs, M. Bar, M. Haser, H. Horn, C. Kolmel, *Chem. Phys. Lett.* **1989**, *162*, 165.
[58] A. D. Becke, *Phys. Rev. A* **1988**, *38*, 3098.
[59] C. Lee, W. Yang, R. G. Parr, *Phys. Rev. B* **1988**, *37*, 785.
[60] S. Grimme, *J. Comput. Chem.* **2006**, *27*, 1787.
[61] E. I. Izgorodina, U. L. Bernard, D. R. MacFarlane, *J. Phys. Chem. A* **2009**, *113*, 7064.
[62] S. Zahn, B. Kirchner, *J. Phys. Chem. A* **2008**, *112*, 8430.
[63] A. E. Reed, R. B. Weinstock, F. Weinhold, *J. Chem. Phys.* **1985**, *83*, 735.
[64] A. E. Reed, L. A. Curtiss, F. Weinhold, *Chem. Rev.* **1988**, *88*, 899.
[65] Gaussian 94 (rev. C.2), M. J. Frisch, G. W. Trucks, H. B. Schlegel, P. M. W. Gill, B. G. Johnson, M. A. Robb, J. R. Cheeseman, T. A. Keith, G. A. Petersson, J. A. Montgomery Jr., K. Raghavachari, M. A. Al-Laham, V. G. Zakrzewski, J. V. Ortiz, J. B. Foresman, J. Cioslowski, B. B. Stefanov, A. Nanayakkara, M. Challacombe, C. Y. Peng, P. Y. Ayala, W. Chen, M. W. Wong, J. L. Andres, E. S. Replogle, R. Gomperts, R. L. Martin, D. J. Fox, J. S. Binkley, D. J. Defrees, J. Baker, J. P. Stewart, M. Head-Gordon, C. Gonzalez, J. A. Pople Gaussian, Inc., Pittsburgh, PA, **1995**.
[66] Gaussian 03 (Revision A.01), M. J. Frisch, G. W. Trucks, H. B. Schlegel, G. E. Scuseria, M. A. Robb, J. R. Cheeseman, J. A. Montgomery Jr., T. Vreven, K. N. Kudin, J. C. Burant, J. M. Millam, S. S. Iyengar, J. Tomasi, V. Barone, B. Mennucci, M. Cossi, G. Scalmani, N. Rega, G. A. Petersson, H. Nakatsuji, M. Hada, M. Ehara, K. Toyota, R. Fukuda, J. Hasegawa, M. Ishida, T. Nakajima, Y. Honda, O. Kitao, H. Nakai, M. Klene, X. Li, J. E. Knox, H. P. Hratchian, J. B. Cross, C. Adamo, J. Jaramillo, R. Gomperts, R. E. Stratmann, O. Yazyev, A. J. Austin, R. Cammi, C. Pomelli, J. W. Ochterski, P. Y. Ayala, K. Morokuma, G. A. Voth, P. Salvador, J. J. Dannenberg, V. G. Zakrzewski, S. Dapprich, A. D. Daniels, M. C. Strain, O. Farkas, D. K. Malick, A. D. Rabuck, K. Raghavachari, J. B. Foresman, J. V. Ortiz, Q. Cui, A. G. Baboul, S. Clifford, J. Cioslowski, B. B. Stefanov, G. Liu, A. Liashenko, P. Piskorz, I. Komaromi, R. L. Martin, D. J. Fox, T. Keith, M. A. Al-Laham, C. Y. Peng, A. Nanayakkara, M. Challacombe, P. M. W. Gill, B. Johnson, W. Chen, M. W. Wong, C. Gonzalez, J. A. Pople, Gaussian, Inc., Pittsburgh, PA, **2004**.
[67] K. R. J. Lovelock, E. F. Smith, A. Deyko, I. J. Villar-Garcia, P. Licence, R. G. Jones, *Chem. Commun.* **2007**, 4866.
[68] *NIST X-ray Photoelectron Spectroscopy Database*, *Version 3.5*, National Institute of Standards and Technology, Gaithersburg, **2003** (http://srdata.nist.gov/xps/NIST).

[69] W. Jiang, Y. T. Wang, T. Y. Yan, G. A. Voth, *J. Phys. Chem. C* **2008**, *112*, 1132.
[70] K. Fumino, A. Wulf, R. Ludwig, *Angew. Chem.* **2008**, *120*, 3890; *Angew. Chem. Int. Ed.* **2008**, *47*, 3830.
[71] R. Lungwitz, V. Strehmel, S. Spange, *New J. Chem.* **2010**, *34*, 1135.
[72] A. Wulf, K. Fumino, R. Ludwig, *Angew. Chem.* **2010**, *122*, 459; *Angew. Chem. Int. Ed.* **2010**, *49*, 449.
[73] P. Bonhôte, A. P. Dias, N. Papageorgiou, K. Kalyanasundaram, M. Gratzel, *Inorg. Chem.* **1996**, *35*, 1168.
[74] U. Gelius, P. F. Heden, J. Hedman, B. J. Lindberg, R. Manne, R. Nordberg, C. Nordling, K. Siegbahn, *Phys. Scr.* **1970**, *2*, 70.
[75] W. F. Egelhoff, Jr., *Surf. Sci. Rep.* **1987**, *6*, 253.
[76] P. H. Citrin, T. D. Thomas, *J. Chem. Phys.* **1972**, *57*, 4446.
[77] J. M. Benson, I. Novak, A. W. Potts, *J. Phys. Chem. B.* **1987**, *20*, 6257.
[78] S. P. Kowalczyk, F. R. Feely, L. Ley, R. A. Pollack, D. A. Shirley, *Phys. Rev. B* **1974**, *9*, 3573.
[79] B. Kirchner, Topics in Current Chemistry, Vol. 290, Springer, **2010**.
[80] P. A. Z. Suarez, S. Einloft, J. E. L. Dullius, R. F. d. Souza, J. Dupont, *J. Chim. Phys.* **1998**, *95*, 1626.
[81] S. A. Katsyuba, T. P. Griaznova, A. VidiŠ, P. J. Dyson, *J. Phys. Chem. B* **2009**, *113*, 5046–5051.
[82] T. Heine, C. Corminboeuf, G. Seifert, *Chem. Rev.* **2005**, *105*, 3889.
[83] K. B. Wiberg, J. D. Hammer, T. A. Keith, K. Zilm, *J. Phys. Chem. A* **1999**, *103*, 21.
[84] A. J. Arduengo, D. A. Dixon, K. K. Kumashiro, C. Lee, W. P. Power, K. W. Zilm, *J. Am. Chem. Soc.* **1994**, *124*, 6361.
[85] M. Hesse, H. Meier, B. Zeeh, in *Spectroscopic Methods in Organic Chemistry*, 2nd ed., Thieme, Stuttgart; New York, **2007**.

Received: April 20, 2010
Published online: July 23, 2010

